forests

MDPI

Article

Effects of Drought on Xylem Anatomy and Water-Use Efficiency of Two Co-Occurring Pine Species

Dario Martin-Benito [1,2,3,*], Kevin J. Anchukaitis [3,4], Michael N. Evans [5], Miren del Río [1,6], Hans Beeckman [7] and Isabel Cañellas [1]

1 Forest Research Centre, (INIA-CIFOR), Ctra. La Coruña km 7.5, 28040 Madrid, Spain; delrio@inia.es (M.d.R); canellas@inia.es (I.C.)
2 Forest Ecology, Department of Environmental Sciences, Swiss Federal Institute of Technology, ETH Zurich, Universitätstrasse 16, 8092 Zürich, Switzerland
3 Tree-ring Laboratory, Lamont-Doherty Earth Observatory of Columbia University, 61 Route 9 W, Palisades, NY 10964, USA
4 School of Geography and Development & Laboratory of Tree-Ring Research, University of Arizona, Tucson, AZ 85721, USA; kanchukaitis@email.arizona.edu
5 Department of Geology and Earth System Science Interdisciplinary Center, University of Maryland, College Park, MD 20742, USA; mnevans@umd.edu
6 Sustainable Forest Management Research Institute, University of Valladolid, INIA Avda, Madrid, s/n, 34004 Palencia, Spain
7 Service of Wood Biology, Royal Museum for Central Africa, Leuvensesteenweg 13, 3080 Tervuren, Belgium; hans.beeckman@africamuseum.be
* Correspondence: dmartin@inia.es or dario.martin@usys.ethz.ch; Tel.: +34913476872

Academic Editor: Giovanna Battipaglia
Received: 4 August 2017; Accepted: 30 August 2017; Published: 8 September 2017

Abstract: Exploring how drought influences growth, performance, and survival in different species is crucial to understanding the impacts of climate change on forest ecosystems. Here, we investigate the responses of two co-occurring pines (*Pinus nigra* and *Pinus sylvestris*) to interannual drought in east-central Spain by dendrochronological and wood anatomical features integrated with isotopic ratios of carbon ($\delta^{13}C$) and oxygen ($\delta^{18}O$) in tree rings. Our results showed that drought induces both species to allocate less carbon to build tracheid cell-walls but increases tracheid lumen diameters, particularly in the transition wood between early and latewood, potentially maximizing hydraulic conductivity but reducing resistance to embolism at a critical phase during the growing season. The thicker cell-wall-to-lumen ratio in *P. nigra* could imply that its xylem may be more resistant to bending stress and drought-induced cavitation than *P. sylvestris*. In contrast, the higher intrinsic water-use efficiency (iWUE) in *P. sylvestris* suggests that it relies more on a water-saving strategy. Our results suggest that narrower cell-walls and reduced growth under drought are not necessarily linked to increased iWUE. At our site *P. nigra* showed a higher growth plasticity, grew faster and was more competitive than *P. sylvestris*. In the long term, these sustained differences in iWUE and anatomical characters could affect forest species performance and composition, particularly under increased drought stress.

Keywords: xylem bending stress; drought; *Pinus*; tracheid; tree ring; water-use efficiency; wood anatomy

1. Introduction

Intense and prolonged drought episodes can significantly affect tree growth and survival, species composition and disturbance dynamics in forests. Increased frequency of these events could potentially affect mortality and recruitment dynamics and lead to changes in distribution and abundance of forest

species [1,2]. Decreased growth and increased mortality under drought conditions might derive primarily from carbon limitation at the source level through stomatal closure and lower carbon assimilation (the carbon-starvation hypothesis [3]) or by reduced meristematic activity and cambial enlargement [4–6], or directly by hydraulic failure [7]. Water deficits can affect the mobilization and transport of carbohydrates reducing growth even if concentrations of soluble carbohydrates increase [4,6,8,9]. Meristematic activity is also reduced during periods of low water availability [4,5]. Xylem development under water-stress conditions is further regulated by complex interactions between these different mechanisms, varying levels of growth hormones, such as auxin or indole acetic acid [10], or changes in carbon allocation patterns [9,11–13].

The response of trees to drought stress varies within a continuum between closing stomata to reduce transpiration to keep xylem water potential within safety margins [14] at the expense of reduced photosynthetic rates (isohydric strategy) [15] or by maintaining similar levels of stomatal conductance but risking increased embolism formation (anisohydric strategy), because stomatal and hydraulic response are closely co-regulated [16]. Xylem safety levels involved in hydraulic failure depend on anatomical characteristics such as pit structure [17,18] and conduit lumen and cell-wall thickness [19]. In the anisohydric *Juniperus thurifera* L., increases in intrinsic water-use efficiency (iWUE) are likely to reduce growth and cell-wall thickness, supporting a partial role of carbon source limitation in the decline of tree vigor and hydraulic resistance [20]. Tree growth rates and drought resistance are closely balanced across many different species and forest ecosystems [21] and adaptations to different environments via these physiological and wood anatomical mechanisms are partly responsible for the distributional limits of conifer species [22].

Under similar levels of drought stress, different species with different functional traits can experience different decline and mortality rates [3], which can result in long-term differences in competitive ability and affect species composition. Several studies in eastern Iberia show a severe drought-induced decline and mortality of *P. sylvestris* L., but not in *P. nigra* Arn. [2,23] or oaks [24], although drought-induced die-back of *P. nigra* has been reported in Italy [25]. Therefore, in the present study, we focus on how *P. sylvestris* and *P. nigra* growing in the same stand perform in response to climate variability and drought. These two species differ in their ecological requirements and distribution ranges. Although *P. nigra* generally shows a higher drought resistance [26] and greater sapling survival [23] than *P. sylvestris*, both pines frequently form mixed stands in Mediterranean mountains [27]. While *P. nigra* is restricted to the mountains surrounding the Mediterranean Basin [27], *P. sylvestris* has a wide circumboreal extension [28]. In east-central Spain, the growth of both *P. nigra and P. sylvestris* is sensitive to climate-mainly summer drought [29]. Although both species sometimes show similar vulnerability to embolism [2], a loss of 50% hydraulic conductivity can occur in *P. nigra* at higher tensions and lower water potentials than *P. sylvestris* (−2.8 MPa [30] vs. −3.20 MPa [2], respectively). It remains essential to increase our knowledge about how functional traits might affect the differential survival and competition ability of coexisting species. Mediterranean forests are already subjected to a high frequency of strong droughts and offer an appropriate system to test the effects of increasing drought frequencies and intensities associated with climate change [31].

Annual growth rings record the response of trees to changes in their environment. Changes in stomatal conductance are recorded in the stable isotopes of wood cellulose [32,33]. Merging dendrochronology, proxies of xylem vulnerability calculated from xylem anatomical features, and the analysis of intrinsic water-use efficiency provides a valuable approach to explore species' and communities' long-term responses to drought [20,25,34]. In the present study, we investigate the effects of drought on plant growth and hydraulic architecture, wood anatomical plasticity, and water-use efficiency under different levels of moisture availability of *P. nigra* and *P. sylvestris* over a 47-year period. The specific objectives of the study are to (1) determine how xylem traits (tracheid wall thickness and lumen diameter) differ between the two pine species and characterize their tree-ring width; (2) investigate how xylem morphology is affected by climatic conditions in years with contrasting water availability; and (3) assess whether different adaptive response to drought of traits and growth

might be favouring one of the two species. We hypothesized that the *P. nigra* will show xylem hydraulic traits typical of more drought tolerant species and lower iWUE that would reflect higher stomatal conductance than *P. sylvestris*. This response would allow *P. nigra* to withstand periods of drought better than *P. sylvestris* but also grow faster under moister conditions.

2. Materials and Methods

2.1. Site Description

Our study area was located in east-central Spain (40°17′ N; 1°59′ W) at an elevation of 1460 m a.s.l. A mixed, even-aged (ca. 90 years old) stand of *Pinus nigra* Ait. (Black pine) and *P. sylvestris* L. (Scots pine) developed on a deep forest soil on calcareous bedrock and a flat slope. All trees analysed in this study were growing within a permanent plot of 2000 m^2 monitored since 1964, which minimizes the influence of the possible differences in microsite and anthropogenic and natural disturbances in all variables analysed. Precipitation and temperature data from a nearby meteorological station (1250 m a.s.l.; 40°13′ N; 1°55′ W; about 10 km southwest of our study site) were provided by the Spanish National Meteorological Agency (AEMET). During the period 1960–2000, climate was characterized by an annual precipitation sum of 924 mm·$year^{-1}$ with two maxima (spring and autumn), 13.3 °C mean temperature, and summer drought during July and August (Figure 1). From monthly precipitation and temperature data, we alculated the multiscalar climatic drought index SPEI (standardized precipitation-evapotranspiration index [35]). Years with an August SPEI for a time scale of 12 months (SPEI12) above (below) one standard deviation were considered wet (dry) (Figure 1). For exploring the responses of xylem traits to extreme dry and wet years, we classified the 47 years of the study as average (n = 29), dry (n = 8) or wet (n = 10).

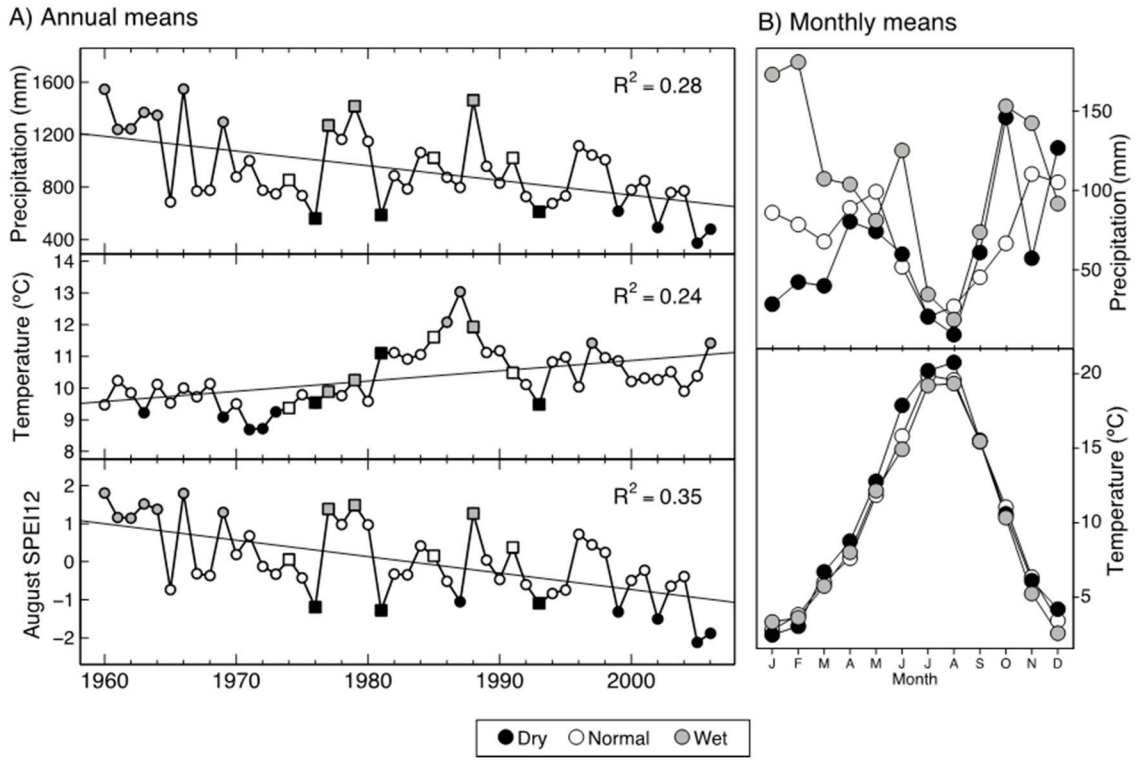

Figure 1. (**A**) Annual total precipitation, mean temperature and August standardized precipitation-evapotranspiration index over 12 months (SPEI12); (**B**) Mean monthly values for precipitation and mean temperature. Solid circles represent annual values, colored based on whether the year was classified as average, wet, or dry. Solid squares represent the nine years selected for isotopic ratio analysis of the annual rings formed those years.

2.2. Dendrochronological and Wood Anatomical Methods

Two cores were extracted from 15 dominant trees of each species within the plot (30 trees in total). Dominance was defined as the 20 largest trees in diameter at breast height (DBH) in the 2000 m^2 plot (i.e., 100 largest trees per hectare). Cores were mounted on grooved boards, sanded and crossdated following standard dendrochronological procedures. The width of each annual ring (TRW), earlywood (EW), and latewood (LW) were measured to the nearest 0.01 mm on a LINTAB measuring stage and the TSAP software [36]. The computer program COFECHA was used to check crossdating and validate measurement quality [37]. A subset of five trees per species highly correlated with their species TRW chronologies were selected for the analysis of their wood anatomical traits and stable isotope ratios (carbon and oxygen). It was later discovered that an extensive defoliation by the pine processionary moth *Thaumetopoea pityocampa* (Denis & Schiffermüller) occurred in these pine forests in 1991 [38], so we exclude data for that year from our analyses. It is worth noting that keeping the results for year 1991 in the analysis or excluding them produced similar results in all analysis performed.

For wood anatomical features, smaller sections (ca. 1–2 cm long) were cut from the cores corresponding to subperiods between 1960–2006 and embedded in polyethylene glycol (1500 MW PEG) blocks [39]. Sections ca. 20 µm thick were cut with a sliding microtome, dehydrated and mounted onto non-permanent glass microscope slides. In certain years, only three or four trees could be used for the anatomical analysis (Figure S1 in supplementary material). In total, we analysed 447 rings (223 for *P. nigra* and 224 for *P. sylvestris*; Figure S1 in supplementary material). Digital images were obtained at a magnification of 40X using a video camera and an optical Nikon Eclipse E600 microscope. To profit from the high image contrast that the autofluorescence of lignin creates under UV light [40], we used UV reflected light from a mercury vapour lamp and a U-MWU Olympus filter. For rings wider than 500 µm, several successive images were blended into a mosaic image before analysis. Lumen diameter (LD), cell-wall thickness (CWT), number of cells (NC) and lumen area (LA) were measured (Figure S2 in supplementary material) along five complete radial rows of cells for each ring using the ImageJ software [41] with a resolution of 1430 pixels/µm. Radial tracheid dimensions were chosen because tangential dimensions are rather constant within and among different growth rings [42].

The cell wall thickness (CWT) of each individual tracheid was calculated as $CWT_i = 0.5 \cdot (CWT_{i-1} + CWT_{i+1})$, where CWT_{i-1} and CWT_{i+1} represent the distance between left ($i-1$) and right ($i + 1$) side tracheid lumen to the specific tracheid (i) (Figure S2 in supplementary material; [43]. For the first and last tracheids in each tree ring, the formula was modified to $CWT_{first} = CWT_{i+1}$ and $CWT_{last} = CWT_{i-1}$. Cells in which $CWT \cdot 4 \geq LD$ were considered as latewood [43]. We also estimated a conduit wall reinforcement or bending stress resistance factor as $(t/b)^2$, where t is the double CWT and b is the side of a hypothetical square conduit of area LA. In this study, we used the bending stress resistance factor [$(t/b)^2$] as a proxy for hydraulic safety from implosion by negative pressure because it is strongly correlated to cavitation resistance [44].

Because cell number differed within and between growth rings (Figure 2), standardized tracheidograms were estimated from the original measurements for each radial file to allow direct comparison between cells in different cell files, rings, and trees. In tracheidograms, all radial files are converted to constant standardized number of cells (25 cells) by a weighted mean of the cell dimension within the file. We chose 25 cells because it was close to the mean number of cells for the rings during the studied period (Figure 2). We briefly describe the process of tracheidogram standardization in supplementary material (for a detailed description of the method see [45]).

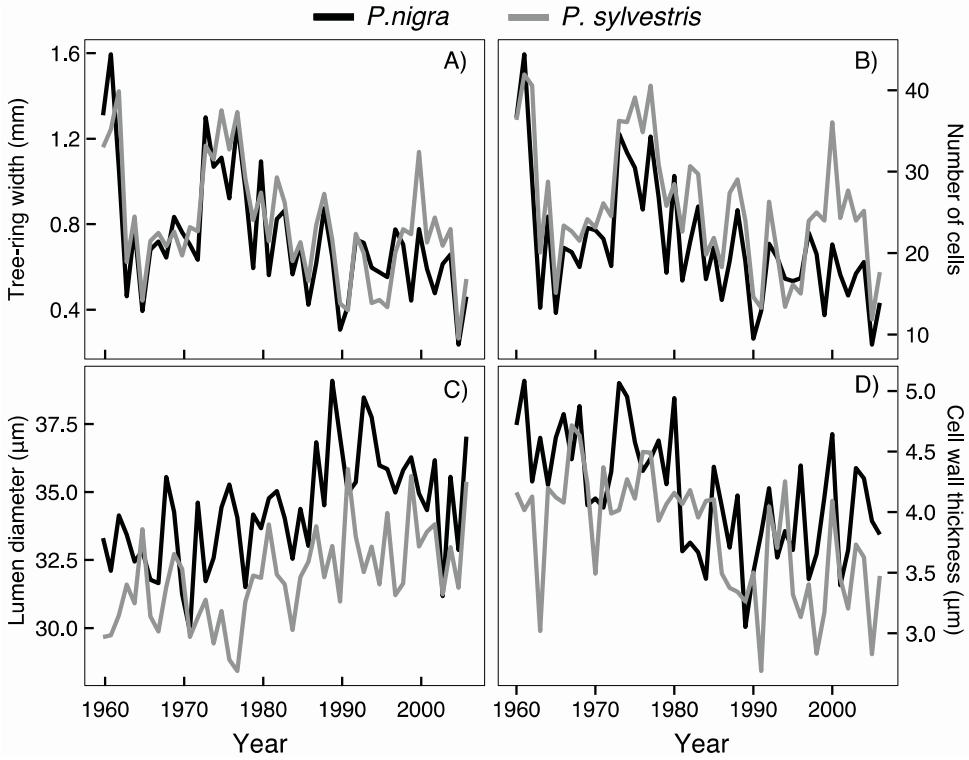

Figure 2. Mean species chronologies for different tree-ring traits and correlation coefficients between species. (**A**) Tree-ring width (r = 0.85, p = <0.001); (**B**) number of cells, (r = 0.86, p =< 0.001); (**C**) tracheid lumen diameter, (r = 0.42, p = 0.004); and (**D**) cell wall thickness (r = 0.46, p = 0.001). Note different scales in the y-axis of the four panels.

2.3. Stable Isotopes

A second core from the same 10 trees used for anatomical analysis was used for carbon and oxygen isotopic analysis. We selected three wet, dry, and average years in the middle of the analysis period for these analyses (Figure 1; wet years: 1977, 1979, 1988; dry years: 1976, 1981, 1993; average years: 1974, 1985, 1991). For these selected nine years (Figure S1 in supplementary material), wood of complete rings including early and latewood was separated and cut into thin slivers under a microscope. We extracted α-cellulose from individual ring samples (i.e., not pooling rings from different trees) following a standard large batch processing procedure [46,47]. From each ring sample, 200 ± 10 µg of α-cellulose were encapsulated in silver foil for the determination of $^{13}C/^{12}C$ and $^{18}O/^{16}O$ isotopic ratios. The carbon and oxygen isotope ratios were determined simultaneously by first converting cellulose to carbon monoxide via pyrolysis at 1080 °C in a Costech elemental analyzer and then measured via a continuous flow Elementar Isoprime mass spectrometer [48]. Carbon isotopic values were expressed in the delta notation as $\delta^{13}C_c$ relative to the standard VPDB (Vienna Pee Dee belemnite):

$$\delta^{13}C_{sample} = \left[\frac{(^{13}C/^{12}C)_{sample}}{(^{13}C/^{12}C)_{VPDB}} - 1\right] \times 1000‰ \quad (1)$$

Oxygen values are expressed as $\delta^{18}O_c$ and referenced to VSMOW (Vienna Standard Mean Ocean Water), using two calibrated cellulose working standards to correct for possible systematic sequential drift, amplitude effects and scale compression by the CF-IRMS system.

$$\delta^{18}O_{sample} = \left[\frac{(^{13}O/^{12}O)_{sample}}{(^{13}O/O)_{VSMOW}} - 1\right] \times 1000‰ \quad (2)$$

The carbon isotope data were converted to carbon isotope discrimination (Δ) as

$$\Delta = \left(\delta^{13}C_a - \delta^{13}C_c\right) / \left(1 + \delta^{13}C_c/1000\right) \quad (3)$$

where $\delta^{13}C_c$ is the isotopic ratio in wood cellulose and $\delta^{13}C_a$ the ratio in atmospheric air [32]. Due to the increase of atmospheric CO_2 inputs from ^{13}C depleted fossil fuels with respect to the pre-industrial atmospheric $\delta^{13}C$ of −6.4‰, Suess effect [49], $\delta^{13}C_c$ was modified by adding the correction values presented by McCarroll and Loader [33]. The standard deviation for replicate measurements of the working standards of isotope ratios for carbon and oxygen were 0.12‰ and 0.26‰, respectively.

From carbon isotopic ratios, we also estimated the intrinsic water-use efficiency (iWUE), i.e., the ratio between net carbon assimilation in photosynthesis (A) and stomatal conductance for water g_w (related to stomatal conductance for CO_2 as g_w = 1.6 g; [32]). This ratio is proportional to ($c_a - c_i$) through the expression

$$\text{iWUE} = \frac{A}{g_w} = \frac{(c_a - c_i)}{1.6} \quad (4)$$

where c_a and c_i are the partial pressure of CO_2 in atmospheric air and in the intercellular space of the pine needle, respectively.

Thus, iWUE can also be estimated from Δ (carbon discrimination) in the tree rings and c_a from [50] as:

$$\text{iWUE} = \frac{c_a \cdot (b - \Delta)}{1.6 \cdot (b - a)} \quad (5)$$

Following the dual-isotope conceptual model of Scheidegger, et al. [51] and the recommendations by Roden and Siegwolf [52], we compared the differences between $\delta^{13}C$ and $\delta^{18}O$ isotopic composition (ΔC and ΔO) observed for dry and wet years with respect to average years for each tree (*i*) and year (*j*). We then averaged per species to obtain composite averages and uncertainties. We analysed these changes in isotopic discrimination in terms of changes in average net photosynthesis (A) and stomatal conductance (g_l).

2.4. Statistical Analysis

We used linear mixed-effects models (LMM) to analyze the contribution of each anatomical feature (i.e., number of cells, cell wall thickness, lumen diameter) to ring width and to explore the response of both pine species to years of differing water availability. In the first case, TRW was modeled by species as a function of cell-wall thickness (CWT), lumen diameter (LD), and number of cells (NC) of earlywood (EW) and latewood (LW) in the form

$$\text{TRW} = a_i \cdot \text{CWT}_{ew} + b_i \cdot \text{CWT}_{lw} + c_i \cdot \text{LD}_{ew} + d_i \cdot \text{LD}_{lw} + e_i \cdot \text{NC}_{ew} + f_i \cdot \text{NC}_{lw} + t_j \quad (6)$$

where a_i–f_i are model fixed parameters for each species *i*, and t_j represents a random intercept of the linear model for each of the 10 trees *j*.

In the second case, the effect of drought on tree growth was analyzed on six dependent variables with the model

$$\textit{Variable}_i = a_i \cdot \textit{Species} + b_i \cdot \textit{SPEI12} + c_i \cdot \textit{Year} + d_i \cdot \textit{Species}\ \text{SPEI12} + t_{j,i} \quad (7)$$

where a_i–d_i are the corresponding model parameters (a–d) for each dependent variable *i*, whereas $t_{i,j}$ represents a random intercept for each of the 10 trees *j* for each model with variable *i*. The six *i* dependent variables considered were ring width, cell-wall thickness, lumen diameter, and number of cells in the entire ring, earlywood, and latewood. The variable *Year* was introduced in the model as a surrogate for age, because all trees were of very similar age, and it allows for the accounting for age trends within the model.

In all cases, trees were included in the models as random effects in order to account for random differences between individuals. LMMs were fitted in R [53] within the nlme package [54] accounting for temporal autocorrelation in the time series and the maximum likelihood (ML), except for estimating the final model, when a restricted maximum likelihood (REML) was used. Models were developed following the successive approach of Zuur et al. [55] from the original set of potential variables (SPEI12, Year, species, and their interactions) and selected based on the corrected Akaike information criterion AICc [56].

In addition, we used the non-parametric Wilcoxon signed-rank test to analyze the possible effects of drought on CWT and LD within the annual ring between years of contrasting water availability for each species. Our null hypothesis was that, for each of the 25 cells along the standardized tracheidogram, cell-wall thickness and lumen distributions have medians that do not differ between dry, wet or average years.

3. Results

3.1. Changes in Climate

Precipitation during the hydrological year (September to August) decreased for the period 1960–2006 at ca. 11.2 mm·year^{-1} (R^2 = 0.29; $p < 0.001$). During the same period, mean annual temperature increased by 0.3 °C per decade (R^2 = 0.24; $p < 0.001$). The highest temperatures were reached in the late 1980s. These precipitation and temperature changes intensified drought as shown by the strong decrease in August SPEI for 12-month periods (R^2 = 0.34; $p < 0.001$). Four of the eight years with SPEI12 below one standard deviation occurred in the last 10 years, whereas seven of the 10 wettest years occurred in the 1960s (Figure 1).

3.2. Interspecific Growth and Anatomical Differences

Average DBH at the moment of sampling was larger *in P. nigra* than in *P. sylvestris* (33.9 ± 54.3 cm vs. 26.2 ± 19.6cm; p = 0.0176; df = 8; Figure S3 in supplementary material) at the same approximate ages. Average ring widths for both species were similar during the study period (p = 0.6019; df = 8) despite *P. sylvestris* having higher number of cells in the earlywood than *P. nigra* (p = 0.0185, df = 8) (Table 1; Figure 2). Cell walls in *P. nigra* were systematically wider in the latewood (p = 0.0195; df = 8; Table 1; Figure 3) and slightly wider in the earlywood (p = 0.0642, df = 8). Black pine also had wider lumen diameter in the earlywood cells (p = 0.0206, df = 8; Table 1; Figure 3).

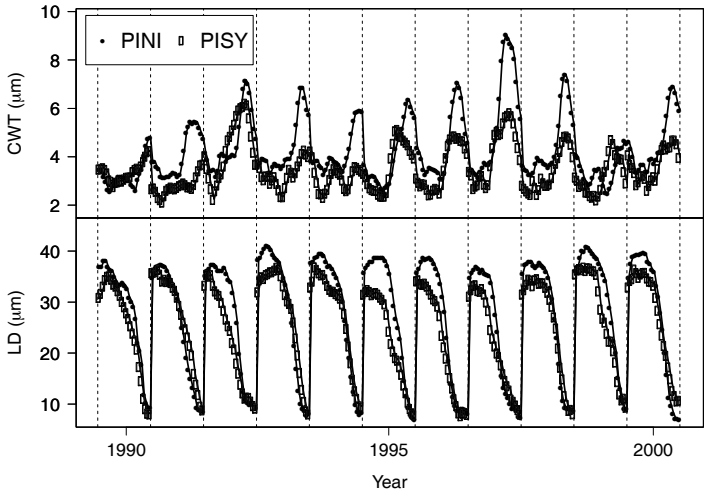

Figure 3. Cell wall thickness (CWT) and lumen diameter (LD) for the normalized tracheidogram of rings formed during the period 1990–2000. Each year represents the mean for 5 trees of each species.

Table 1. Results for the linear mixed-effects models for width of the entire ring, earlywood and latewood, and the total number of cells in the annual ring calculated over the 1960–2006 period. The model fitted was $Variable = a_i \cdot Species + b_i \cdot SPEI12_{Aug} + c_i \cdot Year + d_i \cdot Species \cdot SPEI12_{Aug} + t_{j,i}$, where a_i–d_i are the model parameters (a–d) for each variable *i*, and $t_{i,i}$, represents the random intercept for each of the 10 trees *j* for each variable *i*. $SPEI12_{Aug}$ was treated as a continuous variable. Significant p values at the 5% level are highlighted in bold. EW, earlywood; LW, latewood. Reference species is *P. nigra* which means that positive (negative) parameter estimates for the independent variable "species" need to be considered as increase (decrease) with respect to that species. Data for year 1991 was removed from the analysis.

		Species (*df* = 8)			**SPEI12 (*df* = 423)**			**Year (*df* = 423)**			**Species × SPEI12 (*df* = 423)**		
Variable	**Section**	**Estimate**	**SE**	***p***	**Estimate**	**SE**	***p***	**Estimate**	**SE**	***p***	**Estimate**	**SE**	***p***
Width	Ring	47.67	87.78	0.6019	81.13	23.26	0.0005	−6.71	1.35	<0.0001	−35.85	29.31	0.2220
	EW	51.23	66.05	0.4602	49.27	18.75	0.0089	−6.41	1.10	<0.0001	−21.82	23.60	0.3558
	LW	−3.63	39.49	0.9290	31.84	7.41	<0.0001	−0.29	0.43	0.4924	−13.98	9.33	0.1347
CWT	Ring	−0.35	0.26	0.2046	0.03	0.07	0.9581	−0.02	<0.01	<0.0001	−0.06	0.10	0.4894
	EW	−0.56	0.26	0.0642	0.10	0.04	0.0099	−0.01	<0.01	<0.0001	−0.07	0.05	0.1608
	LW	−1.54	0.53	0.0195	0.30	0.09	0.0009	<0.01	<0.01	0.4976	<−0.01	0.11	0.9985
LD	Ring	−2.48	1.42	0.1190	−0.31	0.24	0.1984	0.06	0.01	<0.0001	0.01	0.30	0.9390
	EW	−4.01	1.39	0.0206	0.30	0.23	0.1964	0.01	0.01	0.3781	0.02	0.30	0.9430
	LW	0.04	0.38	0.9122	0.34	0.11	0.0028	0.01	<0.01	0.0385	0.13	0.14	0.3672
Number of Cells	Ring	4.08	2.67	0.1653	2.23	0.64	0.0006	−0.18	0.04	<0.0001	−0.81	0.82	0.3193
	EW	3.31	1.39	0.0185	1.02	0.43	0.0185	−0.15	0.03	<0.0001	−0.33	0.54	0.5411
	LW	0.77	1.74	0.6695	1.21	0.31	0.0002	−0.03	0.02	0.1561	−0.48	0.40	0.2280

In both species, the number of cells explained over 89% of ring width variability (Table 2; Figure 2). Although *P. sylvestris* had more cells per ring (Figure 2), its ring-width interannual variability was less dependent on the number of cells than *P. nigra* (89.33% and 91.60% respectively; Table 2). Cell wall thickness had a greater influence on ring width in *P. sylvestris* than it did in *P. nigra* (0.074% vs. 0.014%; Table 2). Variability in lumen diameter had a stronger influence on the total ring-width (7.633% and 9.511% for *P. nigra* and *P. sylvestris* respectively) than cell wall thickness (Table 2).

Table 2. Variance in tree-ring width explained (in %) by different anatomical features in its two components (EW, earlywood; LW, latewood) in the mixed effects model $TRW = a_i \cdot CWT_{ew} + b_i \cdot CWT_{lw} + c_i \cdot LD_{ew} + d_i \cdot LD_{lw} + e_i \cdot NC_{ew} + f_i \cdot NC_{lw} + t_j$. All coefficients ($a_i$–$f_i$) were significant at $p = 0.05$ for both species *i*. t_j, represents the intercept for each of the 10 trees *j*. Totals, represent the sum of explained variance by EW and LW of each variable. Data for year 1991 was removed from the analysis.

		P. nigra	*P. sylvestris*
Cell-wall thickness [1]	EW	0.0136	0.0612
	LW	0.0004	0.0123
	Total	0.0140	0.0735
Lumen diameter [1]	EW	2.0721	3.5085
	LW	5.5612	6.0029
	Total	7.6333	9.5113
Number of cells [1]	EW	89.4257	86.7695
	LW	2.1780	2.5628
	Total	91.6037	89.3323
Tree [2]		0.0654	0.0702
Residuals		0.6837	1.0127

[1] model fixed effects; [2]model random effect as different intercept for each of the 10 trees analyzed. The sum of each column equals 100% of variance.

The significant effects of variable *Year* were negative in all cases except for lumen diameter (Table 1). Tree-ring width decreased with age ($p < 0.0001$, $df = 423$), as expected. The number of cells and cell-wall thickness also decreased with age. In contrast, lumen diameter increased ($p < 0.0001$, $df = 423$) (Table 1; Figure 2).

3.3. Effect of Moisture Availability on Tree Growth and Anatomical Traits

Drought (estimated as the index SPEI12) significantly affected most of the growth and xylem parameters analyzed (Table 1). The negative effect of drought on radial growth was more related to a decrease in the number of cells than to cell sizes as indicated by the highly significant coefficients of total ring, EW and LW width and the number of cells in all ring sections (Table 1). Average cell-wall thickness in EW and LW were significantly reduced by drought. Lumen diameter was less influenced by moisture, but lumen in the LW tracheids were also significantly reduced. We found no interaction between species and drought on any of the EW and LW xylem traits.

Because analyzing long time-series can obscure the response of trees to extremes, we also analyzed how ring width and xylem traits responded to extreme wet, dry, and average years (Table 3). Although our previous analysis with SPEI12 as a continuous variable showed no species-drought interactions (i.e., Table 1), discrete extreme years showed significant differences for widths and cell numbers of entire ring, EW, and LW between average, dry, and wet years in *P. nigra* (Table 3, Figure 4). Growth of *P. sylvestris* was higher during wet years but did not differ for dry and average years. Similarly, the differential tracheidograms showed larger reductions of wall thickness in *P. nigra* (up to 30%) during dry years compared to wet years and mainly in the transition zone from EW to LW (Figure 4). Lumen diameter increased in the earlier part of the EW during dry years (Figure 4). Together, these anatomical changes in dry years resulted in tracheids with lower $(t/b)^2$, i.e., resistance to bending stress (Figure 5).

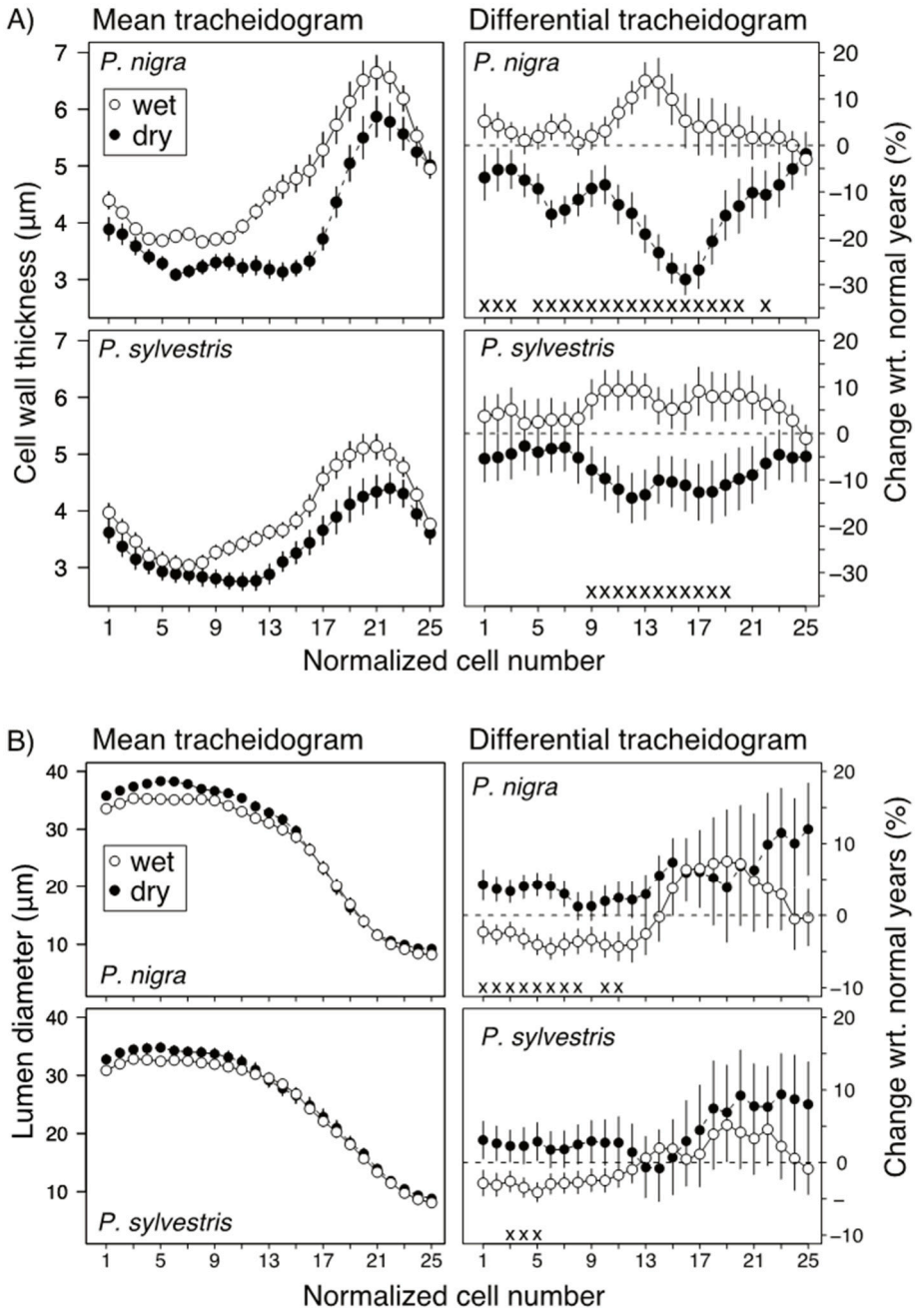

Figure 4. Mean tracheidogram (left panels) and differential tracheidogram (% change with respect to the species average years; right panels) for wet (white circles) and dry (black circles) years for cell-wall thickness (**A**) and lumen diameter (**B**) in *P. nigra* and *P. sylvestris*. Every ring has been normalized to 25 hypothetical cells (see text for details). Vertical bars represent standard error of the mean. Within each species, (x) symbols indicate significant differences ($p < 0.05$) between dry and wet years.

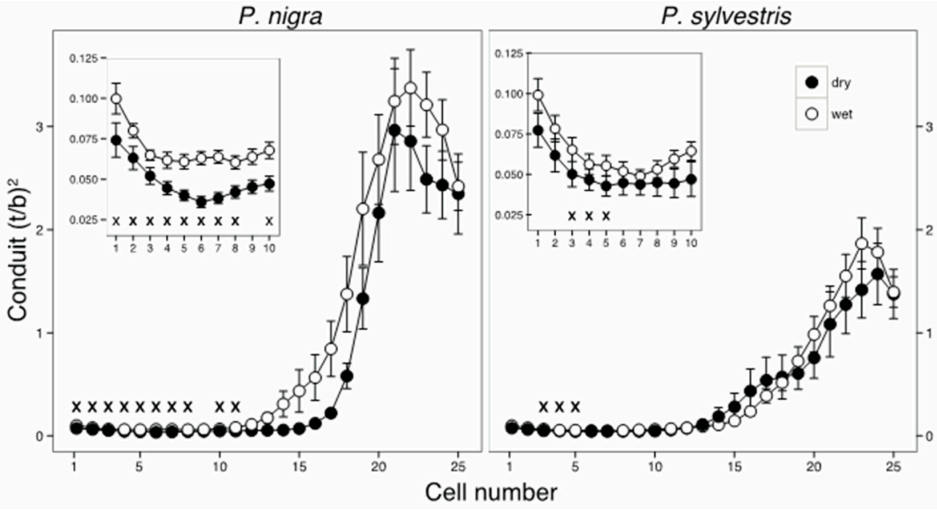

Figure 5. Mean tracheidogram of conduit hydraulic safety (expressed as the $(t/b)^2$ relationship) for *P. nigra* and *P. sylvestris* for dry and wet years. Inset boxes show detail of normalized cells 1 through 10 of each tracheidogram where significant differences between wet and dry years were observed. Vertical bars represent standard error of the mean. Within each species, (x) indicate cells for which hydraulic safety is significantly different ($p < 0.05$) between dry and wet years

Table 3. Wood and tracheid properties in *Pinus nigra* and *P. sylvestris* pine (means and standard deviation) calculated for years with SPEI12 classified as being average, dry or wet for the period 1960–2006. Different letters within a row indicate significant differences at the $p = 0.05$ (except those with * which are significant at the $p = 0.10$) in the linear mixed model approach. EW, earlywood; LW, latewood. Data for year 1991 was removed from the analysis.

		Dry (n = 8)			Average (n = 29)			Wet (n = 10)		
Pinus nigra										
Width (10^{-2} mm)	Ring	555.89	(263.33)	a	727.56	(280.45)	b	948.92	(409.93)	c
	EW	453.82	(201.88)	a	588.27	(219.40	b	749.64	(321.74)	c
	LW	102.07	(80.43)	a *	139.28	(91.54)	b	199.28	(128.00)	c
CWT (µm)	Ring	3.86	(1.15)	a	4.16	(1.12)	ab	4.46	(1.02)	a
	EW	3.30	(0.67)	a	3.79	(0.66)	b	3.97	(0.52)	c
	LW	5.50	(1.81)	a	6.05	(1.46)	a	6.25	(1.58)	a
LD (µm)	Ring	35.93	(4.06)	a	34.19	(3.50)	b	33.40	(3.76)	b
	EW	34.26	(4.43)	a	34.84	(3.24)	a	34.46	(2.73)	a
	LW	7.20	(1.95)	ab	7.14	(1.50)	a	7.80	(1.60)	b
Number of Cells	Ring	16.36	(6.79)	a	20.91	(7.42)	b	26.94	(10.73)	c
	EW	11.09	(4.33)	a	13.93	(4.82)	b	17.64	(6.82)	c
	LW	5.27	(3.19)	a	6.98	(3.64)	b	9.29	(5.17)	c
Pinus sylvestris										
Width (mm)	Ring	733.38	(337.88)	ab	759.36	(334.55)	a	985.78	(441.26)	b
	EW	605.38	(267.78)	a	621.49	(265.14)	a	807.56	(383.84)	b
	LW	127.99	(126.21)	ab	137.87	(122.07)	a	178.22	(126.44)	b*
CWT (µm)	Ring	3.58	(1.07)	a	3.88	(0.99)	a	3.97	(1.05)	a
	EW	3.03	(0.73)	a	3.17	(0.71)	ab	3.40	(0.77)	b*
	LW	4.15	(1.40)	a	4.54	(1.35)	a	4.74	(1.16)	a
LD (µm)	Ring	32.91	(4.63)	a *	31.72	(3.71)	ab	30.77	(3.71)	b*
	EW	30.28	(5.01)	a	30.73	(3.68)	a	30.60	(3.70)	a
	LW	7.29	(1.94)	a	7.14	(1.48)	a	8.15	(1.64)	b*
Number of Cells	Ring	23.75	(9.97)	a	24.54	(10.19)	a	31.07	(12.36)	b
	EW	16.63	(6.56)	a	16.74	(6.18)	a	21.50	(9.01)	b
	LW	7.12	(5.59)	ab	7.81	(5.59)	a	9.56	(5.67)	b

3.4. Stable Isotopes

Ratios of $\delta^{13}C$ were consistently higher (F = 4.916; p = 0.0306) in *P. sylvestris* (−22.69 ± 0.12‰ mean ± SE) than *P. nigra* (−23.1 ± 0.14‰). Accordingly, values of iWUE were significantly higher (F = 4.916; p = 0.0306) for *P. sylvestris* (107.56 ± 1.27 μmol·mol^{-1}, mean ± SE) than *P. nigra* (103.10 ± 1.34 μmol·mol^{-1}) (Figure 6). Mean values of $\delta^{18}O$ were very similar for both species (*P. nigra* 31.85 ± 0.15‰; *P. sylvestris* 31.76 ± 0.27‰; interspecies comparison F = 0.079; p = 0.779). Our analysis of a few discrete years does not allow for the exploration of temporal trends in iWUE. Differences in the carbon and oxygen isotopic ratios between dry, wet or average years were not statistically significant for either species. A dual carbon-oxygen isotope analysis showed small and non-significant reductions of discrimination for both isotopes for wet and dry years alike compared to average years (Figure 7).

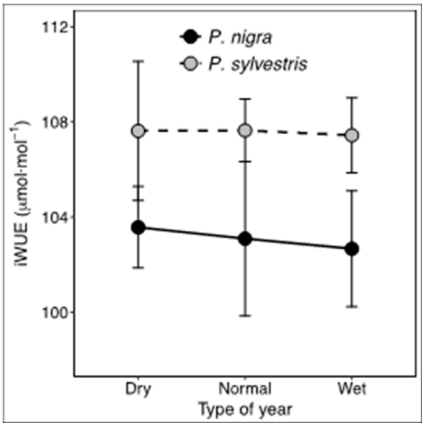

Figure 6. Mean intrinsic water use efficiency (iWUE) for dry, average, and wet years. Each point is the mean of values for three years in five trees per species. Error bars represent the standard error of the mean.

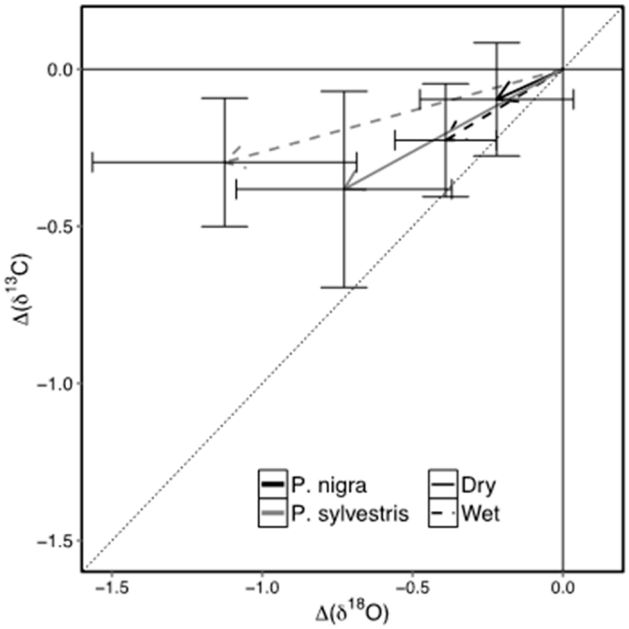

Figure 7. Change of isotopic ratios for carbon [$\Delta(\delta^{13}C)$] and oxygen [$\Delta(\delta^{18}O)$] during dry (solid line) and wet (dashed line) years with respect to the average year for *P. nigra* (black lines) and *P. sylvestris* (grey lines). Each point represents the mean of changes for five trees in three years. Error bars represent the standard error of their respective isotopic ratio change. Dotted diagonal line represents a 1:1 change. Solid vertical and horizontal lines indicate zero anomaly in the dual isotopic model.

4. Discussion

4.1. Effects of Drought on Interannual Radial Growth and Xylem Morphology

In long-lived plants, environmental plasticity in functional traits is vital to assure survival under stress while at the same time remain competitive under more favorable conditions. Our results showed that, in response to drought, both pine species analyzed slowed radial growth and reduced their number of cells and cell-wall thickness, but increased their lumen diameters. This result supports previous findings using simple correlation analysis between anatomical variables and climate [29]. These changes combined may result in increased xylem drought-induced vulnerability, as shown by their lower bending stress resistance $(t/b)^2$. A similar response in *P. sylvestris* was observed in control vs. irrigated [57,58] and precipitation exclusion experiment [59], but are opposite to responses observed in some studies of *P. sylvestris* [13] and other conifers [20,60]. In contrast, our results showed that narrow lumens were produced in LW on dry years particularly in *P. sylvestris* (Table 3), probably as a response to a decline in turgor [13]. The conductivity of tracheids depends partially on the characteristics, number and size of their pits [18,61] as well as their lumen diameter (Hagen-Poiseuille law [62]) and cell wall thickness [19]. The number and diameter of pits in *P. sylvestris* and *P. nigra* increase with lumen diameter [63,64]. A more efficient xylem would result from decreased resistivity due to wider lumens and wider and more abundant pits. Thus, our observations that pines respond to drought by producing fewer tracheids per ring with wider lumens and narrow walls (Tables 1 and 3) suggest that pines build a more efficient xylem while expending less carbon. This carbon-saving strategy or lower allocation to xylem may come at the expense of lower hydraulic strength [59] because larger pits are also more prone to air seeding.

4.2. Intraannual Responses to Drought

Our results show that anatomical responses to drought vary along a growth ring and thus during the growing season. In our study, the effects of drought conditions were minimal at the beginning and at the end of the growing period (Figure 4). The largest anatomical differences between years corresponded to the transition wood (i.e., the ring section between EW and LW), consistent with previous observations [57,58]. Transition wood is most likely formed during late spring or early summer, one of the most critical times of the growing season under Mediterranean climate [65]. As drought stress intensifies during the growing season, xylem development faces varying constrains and may stop completely during the summer, which could lead to bimodal xylogenesis patterns. In some cases, this bimodal pattern may lead to the formation of intra-annual density fluctuations (IADF) if growth stops during the summer drought but resumes latter in the season [65,66]. These flexible xylogenesis patterns grant species higher plasticity by allowing them to concentrate growth during favorable periods. Although several Mediterranean conifers present bimodal xylogenesis, such a pattern has not been observed in *P. sylvestris* [67]. To date, no data exists on *P. nigra* xylogenesis patterns. Focusing our analysis on just EW, LW or on an average for the entire ring would have obscured ecologically important differences. We suggest that studies exploring the ecological functions of wood anatomy should consider at least the transition wood as a separate section, in addition to EW and LW, if higher resolution analyses are not performed.

4.3. Interspecific Responses to Drought

As expected, xylem of *P. nigra* was composed of tracheids with thicker cell walls than *P. sylvestris* and wider lumen diameters in the earlywood (Figures 3 and 4). *P. nigra* also showed higher cell-wall-to-lumen ratios, a driver of wood density, and potentially conferring higher cavitation resistance under low water potentials as suggested by their higher $(t/b)^2$ (Figure 5). Drought, however, induced larger reductions of cell-wall thickness and radial growth in *P. nigra* than it did in *P. sylvestris*. The species with thicker cell-walls, *P. nigra*, might be able to reduce cell−walls more and still maintain higher $(t/b)^2$ than the less drought-adapted species *P. sylvestris* [2,68]. Although conifers

usually keep a large safety margin from drought-induced cavitation [21,61], lower $(t/b)^2$ in *P. nigra* suffering di-back than in healthy trees [25] suggests an important role of bending stress as a partial contributor to hydraulic resistance in tree decline. Low wood density, which is related to $(t/b)^2$ as low cell-wall-to-lumen ratio [44], increases the risk of post-drought dieback in many conifers, including *P. sylvestris* [69,70]. The higher conduit density per unit area in *P. sylvestris* likely contributes to maintaining hydraulic functions in case of xylem cavitation [71]. The wider margin of *P. nigra* to reduce its cell walls during droughts could contribute to the adaptability of this species to variable environmental conditions [23] and could provide a competitive advantage at the study site. Wider tracheid lumens may allow larger hydraulic conductance [61] to support higher stomatal conductance and photosynthesis [72]. Because conifer sapwood may remain functional for multiple years [73], these differences in xylem anatomy may affect tree performance long after the growing season when they are formed.

Narrower cell walls during drought periods may result from changes in carbon allocation towards parts of the plant other than secondary growth. Allocating more carbohydrates to mycorrhiza and root growth, storage or needles [9,11–13] offer the advantage of a faster recovery or the possibility to withstand longer periods of drought and may also be key strategies to ensure survival in long-lived plants [9,70]. Also, *P. nigra* has a higher frequency of rays and parenchyma than *P. sylvestris* [63,64] which are related to higher potential for storing non-structural carbohydrates and water contributing to a faster recovery after stressful conditions [74]. Our result of *P. nigra* reducing wall thickness more than *P. sylvestris* could be due to a greater investment to reserves, defenses or growth of other parts of the plant that allows it to recover better after drought.

Changes of wood anatomical traits in response to drought could vary at different spatial scales of study [26]. At population level, both *P. sylvestris* [63] and *P. nigra* [64] in the Iberian Peninsula develop thick cell-walls and narrow lumens at drier locations. Here, our results suggest that, at interannual scale, the pattern is opposite, i.e., drought induces thinner cell walls but wider lumens, in accordance with results from other species and sites [25,57,58]. The interannual response of hydraulic traits to multiyear climate data, as done in this study, may show different relationships than considering single values of traits, either from single years or averages for several years, across sites differing in mean climatic conditions. The multi-year functionality of sapwood in conifers, the long−term adjustments of leaf/sapwood area ratio (A_l/A_s) to climate, and the alterations of allocation patterns [73] could in part explain these differences. Trees might regulate hydraulic conductance by adjusting for how long sapwood rings remain functional and the architecture of their tracheids at the interannual scale. For example, in dryer climates, where leaf/sapwood area ratio is usually lower [73] and despite their narrower lumens [63,64], trees might attain similar whole-sapwood conductance. Other site-specific factors, invariable at the interannual scale, such as stand density, basal area or soil characteristics could also affect how trees react to climate. Whether these opposing intrasite and intersite variations of xylem traits in response to climate are part of a generalized drought response of conifers requires a systematic review across species and environmental conditions.

4.4. Intrinsic Water-Use Efficiency

Both pine species were expected to show an efficient stomatal control to reduce water loss and prevent high levels of embolism [2,14]. Our dual-isotope analysis, however, suggests that both species reacted by small and non-significant reductions of stomatal conductance (g_s) and net carbon assimilation [51] (Figure 7). Higher iWUE in *P. sylvestris* reflected its tighter stomatal control than *P. nigra* and thus a more isohydric strategy oriented to reduce water spending in accordance with previous results from xeric sites [2,75]. Earlier stomata closing in *P. sylvestris* might contribute to maintaining hydraulic pressure below dangerous levels at this site, but its conservative strategy might reduce its ability to compete for light if *P. nigra* grows taller faster. The possibility exists that the lack of differences in iWUE between different years may be due to isotopic ratios being calculated from EW and LW together, which could mask responses in iWUE at shorter scales, or that drought

during the dry years considered was not enough to trigger a significant stomatal closure even in the most sensitive species. Our results, however, are in line with the lack of interspecific differences reported from tree-rings [2] and sapling needles [23] in these two species. Increased carbon depletion has been suggested to occur in *P. sylvestris* due to its strong stomata closing during droughts [76–78]. Simultaneous reductions of crown growth and lower leaf area index (LAI) [14] during droughts could contribute to maintaining constant levels of iWUE while overall supplying less carbon at the whole-tree level. In fact, pines, including *P. sylvestris* reduced their leaf/sapwood area ratios at dryer and warmer sites [79]. Even considering the potential lag between carbon fixation and use in the secondary cambium [8], our results suggest that narrow cell-walls and reduced growth at interannual scale are not necessarily linked to increased iWUE [20], at least at the drought levels analyzed here. Cambial meristematic activity, shorter enlarging time of tracheid and the number of wall layers produced [58,80] may have played a more important role. A reduction in crown growth or LAI during drought could signal a reduction in cambial growth via lower indole-3-acetic acid (IAA) production [10]. Given future climate change scenarios, we could anticipate a continued coexistence of both species at this site and region under current levels of drought stress with a competition advantage for *P. nigra* given its faster growth and more flexible xylem development.

5. Conclusions

Our analysis of xylem traits showed that both pine species reacted to drought by building a xylem with larger lumens and narrower cell walls which could be more hydraulically efficient while saving carbon resources. The greatest differences in tracheid features between dry and wet years were observed in the transition zone from earlywood to latewood. *Pinus nigra* showed wider lumen and cell walls than *P. sylvestris* as well as higher xylem plasticity to the interannual drought variability (i.e., adjusted more its growth and xylem). The higher iWUE in *P. sylvestris* suggests that it relies more on stomatal control to regulate transpiration. In contrast, the little drought-induced changes in iWUE in both species suggest low levels of drought stress under current climate at the site. Increasing drought conditions, however, could be more detrimental for *P. sylvestris* than for *P. nigra*.

This observed intra-specific response to interannual drought variability contrasts with the general observation that more drought-adapted species, as well as populations from arid sites, produce tracheids with thicker walls and narrower lumens. Results from more species and environments are necessary to further explore whether these opposing trends at different taxonomical and biogeographical scales are generally observed in conifers.

Estimates of forest annual productivity from tree-ring proxies contribute to improving and constraining coupled terrestrial carbon cycle models [81]. Because our results imply a reduction of the amount of carbon per linear unit of radial growth (wood density) in addition to the reduced linear growth, if only tree-ring widths are used for calibration instead of proxies for total carbon storage (e.g., wood density), models may overestimate carbon fixed during drought periods.

Supplementary Materials: The following are available online at www.mdpi.com/1999-4907/8/9/332/s1.

Acknowledgments: We would like to thank Guilermo Gea-Izquierdo (INIA, Spain) for his comments on an earlier version of this article. We acknowledge support to the Fulbright−MICIIN postdoctoral fellowship and Marie-Curie IEF grant (EU-grant 329935) awarded to DMB. DMB and KJA were further supported by NSF grant AGS-1338734. The Instituto Nacional de Investigaciones Agrarias y Alimentarias (INIA) provided funds to maintain the permanent research plot network (Project OT03-002). We also thank the Spanish Meteorological Agency (AEMET) for providing meteorological data. Anonymous reviewers are thanked for critically reading the manuscript and providing feedback that helped improve our manuscript. This is LDEO contribution #8144.

Author Contributions: D.M.-B. conceived and designed the experiments. D.M.-B., K.J.A. and M.N.E. performed the experiments. All authors contributed reagents, materials, and analysis tools. D.M.-B. analyzed the data. All authors wrote the manuscript.

Conflicts of Interest: The authors declare no conflict of interest.

References

1. Anderegg, W.R.L.; Kane, J.M.; Anderegg, L.D.L. Consequences of widespread tree mortality triggered by drought and temperature stress. *Nat. Clim. Chang.* **2013**, *3*, 30–36. [CrossRef]
2. Martínez-Vilalta, J.; Piñol, J. Drought-induced mortality and hydraulic architecture in pine populations of the NE Iberian Peninsula. *For. Ecol. Manag.* **2002**, *161*, 247–256. [CrossRef]
3. McDowell, N.; Pockman, W.T.; Allen, C.D.; Breshears, D.D.; Cobb, N.; Kolb, T.; Plaut, J.; Sperry, J.; West, A.; Williams, D.G.; Yepez, E.A. Mechanisms of plant survival and mortality during drought: Why do some plants survive while others succumb to drought? *New Phytol.* **2008**, *178*, 719–739. [CrossRef] [PubMed]
4. Körner, C. Carbon limitation in trees. *J. Ecol.* **2003**, *91*, 4–17. [CrossRef]
5. Abe, H.; Nakai, T.; Utsumi, Y.; Kagawa, A. Temporal water deficit and wood formation in Cryptomeria japonica. *Tree Physiol.* **2003**, *23*, 859–863. [CrossRef] [PubMed]
6. Körner, C. Paradigm shift in plant growth control. *Curr. Opin. Plant Biol.* **2015**, *25*, 107–114. [CrossRef] [PubMed]
7. Sala, A.; Piper, F.; Hoch, G. Physiological mechanisms of drought-induced tree mortality are far from being resolved. *New Phytol.* **2010**, *186*, 274–281. [CrossRef] [PubMed]
8. Muller, B.; Pantin, F.; Génard, M.; Turc, O.; Freixes, S.; Piques, M.; Gibon, Y. Water deficits uncouple growth from photosynthesis, increase C content, and modify the relationships between C and growth in sink organs. *J. Exp. Bot.* **2011**, *62*, 1715–1729. [CrossRef] [PubMed]
9. Wiley, E.; Helliker, B. A re-evaluation of carbon storage in trees lends greater support for carbon limitation to growth. *New Phytol.* **2012**, *195*, 285–289. [CrossRef] [PubMed]
10. Little, C.H. A.; Savidge, R.A. The role of plant growth regulators in forest tree cambial growth. *Plant Growth Regul.* **1987**, *6*, 137–169. [CrossRef]
11. Dewar, R.C.; Ludlow, A.R.; Dougherty, P.M. Environmental Influences on Carbon Allocation in Pines. *Ecol. Bull.* **1994**, 92–101.
12. Gruber, A.; Pirkebner, D.; Florian, C.; Oberhuber, W. No evidence for depletion of carbohydrate pools in Scots pine (*Pinus sylvestris* L.) under drought stress. *Plant Biol.* **2012**, *14*, 142–148. [CrossRef] [PubMed]
13. Sterck, F.J.; Zweifel, R.; Sass-Klaassen, U.; Chowdhury, Q. Persisting soil drought reduces leaf specific conductivity in Scots pine (*Pinus sylvestris*) and pubescent oak (*Quercus pubescens*). *Tree Physiol.* **2008**, *28*, 529–536. [CrossRef] [PubMed]
14. Irvine, J.; Perks, M.P.; Magnani, F.; Grace, J. The response of *Pinus sylvestris* to drought: Stomatal control of transpiration and hydraulic conductance. *Tree Physiol.* **1998**, *18*, 393–402. [CrossRef] [PubMed]
15. Jones, H. Stomatal control of photosynthesis and transpiration. *J. Exp. Bot.* **1998**, *49*, 387–398. [CrossRef]
16. Martínez-Vilalta, J.; Poyatos, R.; Aguadé, D.; Retana, J.; Mencuccini, M. A new look at water transport regulation in plants. *New Phytol.* **2014**, *204*, 105–115. [CrossRef] [PubMed]
17. Pittermann, J.; Sperry, J.S.; Hacke, U.G.; Wheeler, J.K.; Sikkema, E.H. Inter-tracheid pitting and the hydraulic efficiency of conifer wood: The role of tracheid allometry and cavitation protection. *Am. J. Bot.* **2006**, *93*, 1265–1273. [CrossRef] [PubMed]
18. Choat, B.; Cobb, A.R.; Jansen, S. Structure and function of bordered pits: New discoveries and impacts on whole-plant hydraulic function. *New Phytol.* **2008**, *177*, 608–626. [CrossRef] [PubMed]
19. Pittermann, J.; Sperry, J.S.; Wheeler, J.K.; Hacke, U.G.; Sikkema, E.H. Mechanical reinforcement of tracheids compromises the hydraulic efficiency of conifer xylem. *Plant Cell Environ.* **2006**, *29*, 1618–1628. [CrossRef] [PubMed]
20. Olano, J.M.; Linares, J.C.; Garcia-Cervigon, A.I.; Arzac, A.; Delgado, A.; Rozas, V. Drought-induced increase in water-use efficiency reduces secondary tree growth and tracheid wall thickness in a Mediterranean conifer. *Oecologia* **2014**, *176*, 273–283. [CrossRef] [PubMed]
21. Choat, B.; Jansen, S.; Brodribb, T.J.; Cochard, H.; Delzon, S.; Bhaskar, R.; Bucci, S.J.; Feild, T.S.; Gleason, S.M.; Hacke, U.G.; et al. Global convergence in the vulnerability of forests to drought. *Nature* **2012**, *491*, 752–755. [CrossRef] [PubMed]
22. Brodribb, T.; Hill, R.S. The importance of xylem constraints in the distribution of conifer species. *New Phytol.* **1999**, *143*, 365–372. [CrossRef]

23. Herrero, A.; Castro, J.; Zamora, R.; Delgado-Huertas, A.; Querejeta, J.I. Growth and stable isotope signals associated with drought-related mortality in saplings of two coexisting pine species. *Oecologia* **2013**, *173*, 1613–1624. [CrossRef] [PubMed]
24. Quero, J.L.; Sterck, F.J.; Martínez-Vilalta, J.; Villar, R. Water-use strategies of six co-existing Mediterranean woody species during a summer drought. *Oecologia* **2011**, *166*, 45–57. [CrossRef] [PubMed]
25. Petrucco, L.; Nardini, A.; von Arx, G.; Saurer, M.; Cherubini, P. Isotope signals and anatomical features in tree rings suggest a role for hydraulic strategies in diffuse drought-induced die-back of Pinus nigra. *Tree Physiol.* **2017**, *37*, 523–535. [PubMed]
26. Martinez-Vilalta, J.; Sala, A.; Pinol, J. The hydraulic architecture of Pinaceae—A review. *Plant Ecol.* **2004**, *171*, 3–13. [CrossRef]
27. Barbéro, M.; Losiel, R.; Queézel, P.; Richardson, D.M.; Romane, F. Pines of the Mediterranean Basin. In *Ecology and Biogeography of Pinus*; Richardson, D.M., Ed.; Cambridge University Press: Cambridge, UK, 1998.
28. Nikolov, N.; Helmisaari, H. Silvics of the circumpolar boreal forest tree species. In *A Systems Analysis of the Global Boreal Forest*; Shugart, H.H., Leemans, R., Bonan, G.B., Eds.; Cambridge University Press: Cambridge, UK, 1992; pp. 13–84.
29. Martin-Benito, D.; Beeckman, H.; Cañellas, I. Influence of drought on tree rings and tracheid features of Pinus nigra and Pinus sylvestris in a mesic Mediterranean forest. *Eur. J. For. Res.* **2013**, *132*, 33–45. [CrossRef]
30. Froux, F.; Huc, R.; Ducrey, M.; Dreyer, E. Xylem hydraulic efficiency versus vulnerability in seedlings of four contrasting Mediterranean tree species (*Cedrus atlantica*, *Cupressus sempervirens*, *Pinus halepensis* and *Pinus nigra*). *Ann. For. Sci.* **2002**, *59*, 409–418. [CrossRef]
31. Meehl, G.A.; Tebaldi, C. More Intense, more frequent, and longer lasting heat waves in the 21st century. *Science* **2004**, *305*, 994–997. [CrossRef] [PubMed]
32. Farquhar, G.D.; Ehleringer, J.R.; Hubick, K.T. Carbon Isotope Discrimination and Photosynthesis. *Annu. Rev. Plant. Physiol. Plant Mol. Biol.* **1989**, *40*, 503–537. [CrossRef]
33. McCarroll, D.; Loader, N.J. Stable isotopes in tree rings. *Quat. Sci. Rev.* **2004**, *23*, 771–801. [CrossRef]
34. Beeckman, H. Wood anatomy and trait-based ecology. *IAWA J.* **2016**, *37*, 127–151. [CrossRef]
35. Vicente-Serrano, S.M.; Beguería, S.; López-Moreno, J.I. A multiscalar drought index sensitive to global warming: The standardized precipitation evapotranspiration index. *J. Clim.* **2010**, *23*, 1696–1718. [CrossRef]
36. Rinn, F. *TSAP−Win Professional, Time Series Analysis and Presentation for Dendrochronology and Related Applications*; Version 0.3; Quick Reference; Frank Rinn: Heidelberg, Germany, 2003; p. 20.
37. Holmes, R.L. Computer−assisted quality control in tree-ring dating and measurement. *Tree-Ring Bull.* **1983**, *43*, 69–78.
38. Sangüesa-Barreda, G.; Camarero, J.J.; García-Martín, A.; Hernández, R.; de la Riva, J. Remote-sensing and tree-ring based characterization of forest defoliation and growth loss due to the Mediterranean pine processionary moth. *For. Ecol. Manag.* **2014**, *320*, 171–181. [CrossRef]
39. Schmitz, N.; Verheyden, A.; Kairo, J.G.; Beeckman, H.; Koedam, N. Successive cambia development in *Avicennia marina* (Forssk.) Vierh. is not climatically driven in the seasonal climate at Gazi Bay, Kenya. *Dendrochronologia* **2007**, *25*, 87–96. [CrossRef]
40. Donaldson, L.A. Abnormal lignin distribution in wood from severely drought stressed Pinus radiata trees. *IAWA J.* **2002**, *23*, 161–178. [CrossRef]
41. Rasband, W.S. *ImageJ (1.38x)*; U.S. National Institutes of Health: Bethesda, MD, USA, 1997.
42. Vysotskaya, L.G.; Vaganov, E.A. Components of the variability of radial cell size in tree rings of conifers. *Iawa Bull.* **1989**, *10*, 417–426. [CrossRef]
43. Filion, L.; Cournoyer, L. Variation in wood structure of eastern larch defoliated by the larch sawfly in subarctic Quebec, Can. *Can. J. For. Res.* **1995**, *25*, 1263–1268. [CrossRef]
44. Hacke, U.G.; Sperry, J.S.; Pockman, W.T.; Davis, S.D.; McCulloch, K.A. Trends in wood density and structure are linked to prevention of xylem implosion by negative pressure. *Oecologia* **2001**, *126*, 457–461. [CrossRef] [PubMed]
45. Vaganov, E.A. The tracheidogram method in tree-ring analysis and its application. In *Methods of Dendrochronology*; Cook, E.R., Kairiukstis, L., Eds.; Kluwer: Dordrecht, The Netherlands, 1989; pp. 63–76.
46. Loader, N.J.; Robertson, I.; Barker, A.C.; Switsur, V.R.; Waterhouse, J.S. An improved technique for the batch processing of small wholewood samples to α-cellulose. *Chem. Geol.* **1997**, *136*, 313–317. [CrossRef]

47. Wieloch, T.; Helle, G.; Heinrich, I.; Voigt, M.; Schyma, P. A novel device for batch-wise isolation of α-cellulose from small−amount wholewood samples. *Dendrochronologia* **2011**, *29*, 115–117. [CrossRef]
48. Evans, M.N.; Selmer, K.J.; Breeden, B.T.; Lopatka, A.S.; Plummer, R.E. Correction algorithm for on-line continuous flow stable isotope analyses. *G^3* **2016**, *17*, 3580–3588.
49. Keeling, C.D. The Suess effect: 13Carbon−14Carbon interrelations. *Environ. Int.* **1979**, *2*, 229–300. [CrossRef]
50. McCarroll, D.; Gagen, M.H.; Loader, N.J.; Robertson, I.; Anchukaitis, K.J.; Los, S.; Young, G.H.F.; Jalkanen, R.; Kirchhefer, A.; Waterhouse, J.S. Correction of tree ring stable carbon isotope chronologies for changes in the carbon dioxide content of the atmosphere. *Geochim. Cosmochim. Acta* **2009**, *73*, 1539–1547. [CrossRef]
51. Scheidegger, Y.; Saurer, M.; Bahn, M.; Siegwolf, R. Linking stable oxygen and carbon isotopes with stomatal conductance and photosynthetic capacity: A conceptual model. *Oecologia* **2000**, *125*, 350–357. [CrossRef] [PubMed]
52. Roden, J.; Siegwolf, R. Is the dual-isotope conceptual model fully operational? *Tree Physiol.* **2012**, *32*, 1179–1182. [CrossRef] [PubMed]
53. R Development Core Team. R: A Language and Environment for Statistical Computing. R Foundation for Statistical Computing: Vienna, Austria. Available online: http://www.r-project.org/ (accessed on 18 January 2016).
54. Pinheiro, J.; Bates, D.; DebRoy, S.; Sarkar, D. nlme: Linear and Nonlinear Mixed Effects Models. R Package Version 3.1-128. Available online: http://CRAN.R-project.org/package=nlme (accessed on 1 December 2016).
55. Zuur, A.F.; Ieno, E.N.; Walker, N.J.; Saveliev, A.A.; Smith, G.M. *Mixed Effects Models and Extensions in Ecology with R*; Springer: New York, NY, USA, 2009.
56. Burnham, K.P.; Anderson, D.R. Information theory and log-likelihood models: A basis for model selection and Inference. In *Model Selection and Multimodel Inference: A Practical Information−Theoretic Approach*; Springer: New York, NY, USA, 2002; pp. 33–74.
57. Eilmann, B.; Zweifel, R.; Buchmann, N.; Fonti, P.; Rigling, A. Drought-induced adaptation of the xylem in Scots pine and pubescent oak. *Tree Physiol.* **2009**, *29*, 1011–1020. [CrossRef] [PubMed]
58. Eilmann, B.; Zweifel, R.; Buchmann, N.; Graf Pannatier, E.; Rigling, A. Drought alters timing, quantity, and quality of wood formation in Scots pine. *J. Exp. Bot.* **2011**, *62*, 2763–2771. [CrossRef] [PubMed]
59. Fernández-de-Uña, L.; Rossi, S.; Aranda, I.; Fonti, P.; González-González, B.D.; Cañellas, I.; Gea-Izquierdo, G. Xylem and Leaf Functional Adjustments to Drought in Pinus sylvestris and Quercus pyrenaica at Their Elevational Boundary. *Front. Plant. Sci.* **2017**, *8*, 1200. [CrossRef] [PubMed]
60. Rossi, S.; Simard, S.; Rathgeber, C.; Deslauriers, A.; De Zan, C. Effects of a 20-day-long dry period on cambial and apical meristem growth in *Abies balsamea* seedlings. *Trees* **2009**, *23*, 85–93. [CrossRef]
61. Sperry, J.S.; Hacke, U.G.; Pittermann, J. Size and function in conifer tracheids and angiosperm vessels. *Am. J. Bot.* **2006**, *93*, 1490–1500. [CrossRef] [PubMed]
62. Tyree, M.T.; Zimmermann, M.H. *Xylem Structure and the Ascent of Sap*; Springer: New York, NY, USA, 2002.
63. Esteban, L.; Martín, J.; de Palacios, P.; Fernández, F. Influence of region of provenance and climate factors on wood anatomical traits of Pinus nigra Arn. subsp. salzmannii. *Eur. J. For. Res.* **2012**, *131*, 633–645. [CrossRef]
64. Martín, J.; Esteban, L.; de Palacios, P.; Fernández, F. Variation in wood anatomical traits of *Pinus sylvestris* L. between Spanish regions of provenance. *Trees* **2010**, *24*, 1017–1028. [CrossRef]
65. Wilkinson, S.; Ogée, J.; Domec, J.-C.; Rayment, M.; Wingate, L. Biophysical modelling of intra-ring variations in tracheid features and wood density of *Pinus pinaster* trees exposed to seasonal droughts. *Tree Physiol.* **2017**, *35*, 305–318. [CrossRef] [PubMed]
66. De Micco, V.; Saurer, M.; Aronne, G.; Tognetti, R.; Cherubini, P. Variations of wood anatomy and $\delta^{13}C$ within-tree rings of coastal *Pinus pinaster* showing intra-annual density fluctuations. *IAWA J.* **2007**, *28*, 61–74. [CrossRef]
67. Camarero, J.J.; Olano, J.M.; Parras, A. Plastic bimodal xylogenesis in conifers from continental Mediterranean climates. *New Phytol.* **2010**, *185*, 471–480. [CrossRef] [PubMed]
68. Lebourgeois, F.; Levy, G.; Aussenac, G.; Clerc, B.; Willm, F. Influence of soil drying on leaf water potential, photoshyntesis, stomatal conductance and growth in two black pine varieties. *Ann. For. Sci.* **1998**, *55*, 287–299. [CrossRef]
69. Voltas, J.; Camarero, J.J.; Carulla, D.; Aguilera, M.; Ortiz, A.; Ferrio, J.P. A retrospective, dual-isotope approach reveals individual predispositions to winter-drought induced tree dieback in the southernmost distribution limit of Scots pine. *Plant Cell Environ.* **2013**, *36*, 1435–1448. [CrossRef] [PubMed]

70. Hentschel, R.; Rosner, S.; Kayler, Z.E.; Andreassen, K.; Børja, I.; Solberg, S.; Tveito, O.E.; Priesack, E.; Gessler, A. Norway spruce physiological and anatomical predisposition to dieback. *For. Ecol. Manag.* **2014**, *322*, 27–36. [CrossRef]
71. Robert, E.M. R.; Koedam, N.; Beeckman, H.; Schmitz, N. A safe hydraulic architecture as wood anatomical explanation for the difference in distribution of the mangroves Avicennia and Rhizophora. *Funct. Ecol.* **2009**, *23*, 649–657. [CrossRef]
72. Zhang, J.-L.; Cao, K.-F. Stem hydraulics mediates leaf water status, carbon gain, nutrient use efficiencies and plant growth rates across dipterocarp species. *Funct. Ecol.* **2009**, *23*, 658–667. [CrossRef]
73. Delucia, E.H.; Maherali, H.; Carey, E.V. Climate-driven changes in biomass allocation in pines. *Glob. Chang. Biol.* **2000**, *6*, 587–593. [CrossRef]
74. McDowell, N.G. Mechanisms linking drought, hydraulics, carbon metabolism, and vegetation mortality. *Plant Physiol.* **2011**, *155*, 1051–1059. [CrossRef] [PubMed]
75. Lévesque, M.; Siegwolf, R.; Saurer, M.; Eilmann, B.; Rigling, A. Increased water-use efficiency does not lead to enhanced tree growth under xeric and mesic conditions. *New Phytol.* **2014**, *203*, 94–109. [CrossRef] [PubMed]
76. Aguadé, D.; Poyatos, R.; Rosas, T.; Martínez-Vilalta, J. Comparative drought responses of *Quercus ilex* L. and Pinus sylvestris L. in a montane forest undergoing a vegetation shift. *Forests* **2015**, *6*, 2505–2529. [CrossRef]
77. Galiano, L.; Martínez-Vilalta, J.; Lloret, F. Drought-induced multifactor decline of Scots pine in the Pyrenees and potential vegetation change by the expansion of co-occurring oak species. *Ecosystems* **2010**, *13*, 978–991. [CrossRef]
78. Poyatos, R.; Aguade, D.; Galiano, L.; Mencuccini, M.; Martinez-Vilalta, J. Drought-induced defoliation and long periods of near-zero gas exchange play a key role in accentuating metabolic decline of Scots pine. *New Phytol.* **2013**, *200*, 388–401. [CrossRef] [PubMed]
79. Mencuccini, M.; Bonosi, L. Leaf/sapwood area ratios in Scots pine show acclimation across Europe. *Can. J. For. Res.* **2001**, *31*, 442–456. [CrossRef]
80. Gruber, A.; Strobl, S.; Veit, B.; Oberhuber, W. Impact of drought on the temporal dynamics of wood formation in *Pinus sylvestris*. *Tree. Physiol.* **2010**, *30*, 490–501. [CrossRef] [PubMed]
81. Belmecheri, S.; Maxwell, R.S.; Taylor, A.H.; Davis, K.J.; Freeman, K.H.; Munger, W.J. Tree-ring $\delta^{13}C$ tracks flux tower ecosystem productivity estimates in a NE temperate forest. *Environ. Res. Lett.* **2014**, *9*, 074011. [CrossRef]

© 2017 by the authors. Licensee MDPI, Basel, Switzerland. This article is an open access article distributed under the terms and conditions of the Creative Commons Attribution (CC BY) license (http://creativecommons.org/licenses/by/4.0/).